Pharm Res (2013) 30:1813–1823
DOI 10.1007/s11095-013-1025-4

RESEARCH PAPER

Brain Delivery of NAP with PEG-PLGA Nanoparticles Modified with Phage Display Peptides

Jingwei Li • Chi Zhang • Jing Li • Li Fan • Xinguo Jiang • Jun Chen • Zhiqing Pang • Qizhi Zhang

Received: 12 October 2012 / Accepted: 12 March 2013 / Published online: 3 April 2013

ABSTRACT

Purpose A phage-displayed peptide TGN was used as a targeting motif to help the delivery of NAP-loaded nanoparticles across the blood–brain barrier (BBB), which sets an obstacle for brain delivery of NAP *in vivo*.

Methods Intracerebroventricular injection of $A\beta_{1\text{-}40}$ into mice was used to construct *in vivo* model of Alzheimer's disease. The water maze task was performed to evaluate the effects of the NAP formulations on learning and memory deficits in mice. The neuroprotective effect was tested by detecting acetylcholinesterase (AChE) and choline acetyltransferase (ChAT) activity and conducting histological assays.

Results Intravenous administration of NAP-loaded TGN modified nanoparticles (TGN-NP/NAP) has shown better improvement in spatial learning than NAP solution and NAP-loaded nanoparticles in Morris water maze experiment. The crossing number of the mice with memory deficits recovered after treatment with TGN-NP/NAP in a dose dependent manner. Similar results were also observed in AChE and ChAT activity. No morphological damage and no detectable Aβ plaques were found in mice hippocampus and cortex treated with TGN-NP/NAP.

Conclusions TGN modified nanoparticles could be a promising drug delivery system for peptide and protein drug such as NAP to enter the brain and play the therapeutic role.

J. Li • C. Zhang • J. Li • L. Fan • X. Jiang • J. Chen • Z. Pang • Q. Zhang (✉)
Department of Pharmaceutics, School of Pharmacy, Fudan University
826 Zhangheng Rd.
Shanghai 201203, People's Republic of China
e-mail: qzzhang70@yahoo.com.cn

J. Li • C. Zhang • J. Li • L. Fan • X. Jiang • J. Chen • Z. Pang
Key Laboratory of Smart Drug Delivery
Ministry of Education & PLA
Shanghai, People's Republic of China 201203

KEY WORDS biodegradable nanoparticles · blood–brain barrier (BBB) · brain delivery · NAP

ABBREVIATION

AChE	Acetylcholinesterase
AD	Alzheimer's disease
ADNP	Activity-dependent neuroprotective protein
BBB	Blood–brain-barrier
ChAT	Cholineacetyltransferase
DLC	Drug loading capacity
DLS	Dynamic light scattering
EE	Encapsulation efficiency
NP	Nanoparticles
PEG-PLGA	Poly (ethyleneglycol) - poly (DL-lactide-co-glycolide)
PLGA	Lactic-*co*-glycolic acid
TEM	Transmission electron microscope

INTRODUCTION

Alzheimer's disease (AD) is one of common progressive neurodegenerative diseases and more than 10% of people over 65 have AD (1). The harm of this disease is increasingly prominent with the aging of the human society. In addition, AD also presents the youth oriented tendency in recent years. AD has brought a great influence and pressure to the patients and their family and even the whole society. Therefore, the treatment of AD has become an important problem to be resolved.

The neuroprotective effect of many peptide and protein drugs (e.g., nerve growth factor, brain-derived neurotrophic factor, and basic fibroblast growth factor) has been reported to bring hopes to neurodegenerative diseases such as AD (2–5).

Among them, a novel active peptide NAP (NAPVSIPQ) was identified as a highly active fragment of activity-dependent neuroprotective protein (ADNP), which is essential for brain development (6–8). NAP could offer neuroprotective effects to various neurodegeneration models *in vitro* and *in vivo* (9,10), and also provide neuroprotection in apolipoprotein E deficiency, cholinergic toxicity, closed head injury, stroke, middle aged anxiety and cognitive dysfunction (9,11–15). It was reported that NAP could be a promising candidate for AD therapy (16).

However, due to the poor stability, enzymatic degradation and short blood half-life *in vivo*, along with the presence of the blood–brain barrier (BBB), the brain delivery of protein drugs like NAP which is of great value for their clinical research and application becomes difficult.

Among the strategies to enhance drug delivery across the BBB, the most successful and promising one is to deliver drugs into the brain by receptor mediated transcytosis. Motifs like transferrin, insulin or OX26 can mediate drug transport into the brain by interacting with their corresponding receptors on BBB. Regretfully, transferrin and insulin are endogenous ligands, while OX26 is the mouse monoclonal antibodies against rat transferring receptor. To solve the problem of endogenous saturation and immunogenicity of these existing brain-targeting motifs, a high-throughput screening method called phage display technology was employed for new brain-targeting motif searching. A motif of TGNYKALHPHNG (denoted as TGN) was obtained in our previous study (17). TGN could facilitate polyethylene glycol-polylactide-polyglycolide (PEG-PLGA) nanoparticles across the BBB, leading to significant higher bEnd.3 cells uptake and *in vivo* brain accumulation (17). However, no drug was loaded on this delivery system in the previous study. Whether TGN conjugated PEG-PLGA nanaoparticles could enhance the penetration of peptide drugs such as NAP through BBB and exert their neuroprotective effect on AD *in vivo* still remains to be further studied.

In this study, TGN was conjugated with PEG-PLGA nanoparticles to construct a brain-targeting nanocarrier (TGN-NP) to deliver NAP into the central nervous system. We hypothesized that NAP entrapped in TGN-NP could have better neuroprotective effect than NAP alone. To test our hypothesis, we used $A\beta_{1\text{-}40}$ aggregate injection for the building of Alzheimer's disease model. Then the neuroprotective effect of TGN-NP/NAP was evaluated by Morris water maze task, tissue histology and activity of acetylcholinesterase (AChE) and choline acetyltransferase (ChAT).

MATERIALS AND METHODS

Materials and Animals

Methoxy-poly (ethyleneglycol)-Poly (lactic-*co*-glycolic acid) (MePEG3000-PLGA40000 (25:75)) and Maleimide-poly (ethyleneglycol)-Poly (lactic-*co*-glycolic acid) (Mal-PEG3400-PLGA40000 (25:75)) were synthesized by University of Electronic Science and Technology of China. TGN (TGNYKALHPHNGC) and NAP (NAPVSIPQ) were synthesized by the Chinese Peptide Company (China). β-amyloid 1–40 (Aβ1-40) was obtained from Sigma-Aldrich Chemical Co. (St. Louis, MO, US). Quantity Protein assay kits, AChE and ChAT activity assay kits were purchased from Nanjing Jiancheng Bioengineering Institute (Nanjing, China). All the other chemicals were of analytical reagent grades.

ICR mice (25–30 g) were obtained from Shanghai Sino-British Sippr/BK Lab Animial Ltd. (Shanghai, China) and maintained at a constant temperature (25 ± 1°C) on a 12 h light–dark cycle with access to food and water *ad libitum*. The animal studies were carried out according to the protocols approved by the ethical committee of Fudan University.

Preparation and Characterization of TGN-NP/NAP

PEG-PLGA nanoparticles loaded with NAP (NP/NAP) were prepared with a blend of Maleimide-PEG-PLGA and MePEG-PLGA using double emulsion/solvent evaporation technique as described previously (17). Briefly, 20 mg of MePEG-PLGA and 5 mg of Maleimide-PEG-PLGA were dissolved in 1 mL of dichlormethane. With 50 μL NAP solution (5 mg/mL) as the inner water phase, the w/o primary emulsion was produced in an ice-water bath by sonication (120 W, 30 s). Then the primary emulsion was sonicated in 2 mL of 1% aqueous sodium cholate solution at 200 W for 30 s to obtain the w/o/w emulsion. The emulsion was further diluted into 20 mL of a 0.5% sodium cholate solution and stirred for 5 min. The organic solvent was evaporated by rotary vacuum. Then the NPs were collected by centrifugation at 12,000 rpm for 45 min at 4°C and washed three times with deinoized water to remove the NAP unentrapped.

NP/NAP modified with TGN (TGN-NP/NAP) was prepared by maleimide-thiol coupling reaction at room temperature for 8 h, with the molar ratio of thiol of TGN to maleimide being 1:3. The obtained products were further eluted with 0.01 M phosphate buffered saline buffer (PBS, pH 7.4) through sepharose CL-4B column to remove the unconjugated TGN.

The morphological examination was carried out using transmission electron microscope (TEM) (H-600, Hitachi, Japan). The mean diameter and zeta potential of the nanoparticles were determined by dynamic light scattering (DLS) using a Zeta Potential/Particle Sizer NIC-OMPTM 380 ZLS (PSS.NICOMP PARTICLE SIZE SYSTEM, Santa Barbara, CA).

Determination of Encapsulation Efficiency and Loading Capacity of TGN-NP/NAP

For the determination of encapsulation efficiency, 25 μL of NP/NAP (25 mg/mL) was dissolved in 60 μL of acetonitrile to release NAP from the nanoparticles. Then 120 μL of 0.1% (v/v) trifluoroacetic acid was added to precipitate the polymers. After centrifugation at 12,000 rpm for 30 min, 20 μL of the supernatant was injected into an HPLC system to detect the level of NAP entrapped in NPs. The measurement was performed with a 15 min linear gradient elution of 0. 1% trifluoroacetic acid in acetonitrile (solvent B) and 0. 1% trifluoroacetic acid in water (solvent A) by RP-HPLC (Dikma Diamonsil® C18, 250×4.6 mm, 5 μm). The flow rate was 1 mL/min, with the mobile phase starting from 85% solvent A and 15% solvent B to 60% solvent A and 40% solvent B. The drug encapsulation efficiency and loading efficiency were calculated as indicated below.

$$\text{Encapsulation effiency (\%)} = \frac{\text{amount of NAP in nanoparticels}}{\text{total amount of NAP added initially}} \times 100\%$$

$$\text{Loading capacity (\%)} = \frac{\text{amount of NAP in nanoparticels}}{\text{nanoparticles weight}} \times 100\%$$

Neuroprotection Effects of the NAP Formulations on $A\beta_{1\text{-}40}$-Induced Alzheimer's Disease Model

In Vivo Model of Alzheimer's Disease

Ryuichi *et al.* have demonstrated that intracerebroventricular injection of $A\beta_{1\text{-}40}$ into mice can significantly cause specific dysfunction of memory processes (18), and this validated animal model could be useful to develop and evaluate potential drugs for AD. In brief, $A\beta_{1\text{-}40}$ was dissolved in saline (1 mg/mL) and incubated at 37°C for 7 consecutive days for aggregation. Before surgery, mice were anaesthetized by i.p. of 5% chloral hydrate and fixed in a David Krof stereotaxic apparatus. Five microliters of $A\beta_{1\text{-}40}$ was subsequently injected slowly into bilateral hippocampus (±1.8 mm lateral to the midline, 2.3 mm posterior to the bregma and 2.0 mm ventral to the skull surface) within 6 min. The needle was left in the place for another 5 min before it was slowly withdrawn. Sham-operated animals were injected with saline of the same volume.

Drug Administration and Experimental Design

Mice were divided into eleven groups (Table I): three control groups (Group A-C) and eight test groups (Group D-K). The formulations were given to the mice according to the table for seven consecutive days, and Morris water maze test was carried out from the eighth day.

Table I Groups and Treatments

Groups	Group name	Administration for 7 days
A	Normal control	i.v. 100 μL saline
B	AD model control	i.v. 100 μL saline
C	Sham-operated control	i.v. 100 μL saline
D	NAP solution i.v.	i.v. 2 μg/kg NAP solution
E	NAP solution s.c. (low dose)	s.c. 2 μg/kg NAP solution
F	NAP solution s.c. (high dose)	s.c. 10 μg/kg NAP solution
G	NP/NAP i.v. (low dose)	i.v. 2 μg/kg NP/NAP
H	NP/NAP i.v. (high dose)	i.v. 4 μg/kg NP/NAP
I	TGN-NP/NAP i.v. (low dose)	i.v. 1 μg/kg TGN-NP/NAP
J	TGN-NP/NAP i.v. (medial dose)	i.v. 2 μg/kg TGN-NP/NAP
K	TGN-NP/NAP i.v. (high dose)	i.v. 4 μg/kg TGN-NP/NAP

Morris Water Maze Test

The Morris water maze test was conducted in a circular tank of 120 cm diameter and 50 cm depth, filled with black-painted water at a temperature of 25±1°C. The tank was divided into four equal quadrants. A hidden platform (9 cm in diameter) was submerged 2 cm below the water surface in the center of the northwest quadrant. The water tank was placed in a test room in which there were several unchanged cues external to the maze throughout the water maze test. The swimming paths of mice were tracked with the use of the camera fixed on the ceiling of the room.

The procedure of the Morris water maze consisted of a five-day training session and a probe trail on the fifth day. Formulations or saline were administrated 60 min prior to the first trial of each day. In training session, mice were tested four times daily, released from four starting points in a random manner and allowed to swim for 60 s. Each mouse was allowed to rest for 30 s on the condition of mounting the platform within 60 s. If the mouse failed to find the platform within 60 s, it was guided to the platform by the experimenter and placed there for 30 s.

A single probe trail was performed 60 min after last training trail. The hidden platform was removed and the mice were released from the center of the edge of southeast quadrant and allowed to swim for 60 s. The time spent in the target quadrant and the number of times crossing the area where the platform had been located during the training were recorded for each mouse.

Measurement of AChE and ChAT Activity in Mouse Hippocampus and Cortex

The mice were sacrificed by decapitation after the Morris water maze test, and hippocampus and cortex tissues were isolated from the brain and homogenized in ice-cold saline. The supernatant was obtained after centrifugation at

4000 rpm for 30 min at 4°C. Acetylcholinesterase (AChE) and choline acetyltransferase (ChAT) activity was determined spectrophotometrically with the use of the assay kit according to the manufacturer's protocols. The protein concentration was measured with the Quantity Protein assay kit. The activity of the enzymes was expressed as units of enzyme per g protein.

Histology

The mice were anaesthetized with chloral hydrate after behavioral studies, and transcardially perfused with saline followed by 4% paraformaldehyde solution. The whole brain was dissected and fixed in 4% paraformaldehyde solution overnight before dehydration. Then the brain was embedded in paraffin, and the thin sections (6 μm) were cut from the injection site, mounted onto slides for haematoxylin–eosin (HE) staining and Congo red staining.

Statistical Analysis

All data were expressed as mean ± S.E.M. Statistical differences were determined by one-way ANOVA, followed by *Post hoc* analysis of Dunnett for multi-group comparison. Student's *t*-test was used for two-group comparison and $p<0.05$ was considered statistically significance.

RESULTS

Preparation and Characterization of TGN-NP/NAP

Nanoparticles were prepared using the emulsion/solvent evaporation method. The nanoparticles were spherical and uniform under transmission electron microscope (Fig. 1). The particle sizes were 132 nm and 151 nm, and the zeta potentials were −21.42 mV and −19.59 mV for NP/NAP and TGN-NP/NAP, respectively. A slight diameter increase was observed after the conjugation with TGN, and the negative charge of TGN-NP/NAP was lower than that of NP/NAP.

The encapsulation efficiency and loading capacity of NP/NAP and TGN-NP/NAP were 57.52% and 48.18%, 0.67% and 0.58%, respectively.

Neuroprotection Effects of the NAP Formulations on $A\beta_{1\text{-}40}$-Induced Alzheimer's Disease Model

Morris Water Maze Test

The water maze performance was used to evaluate the effects of the NAP formulations on learning and memory deficits in mice. Figure 2a shows the mean escape latency during the five-day training session. All groups of mice displayed a reduction in the escape latency. From the second day, the latency of AD control group was significantly longer than that of Normal and Sham-operated groups, indicating that intracerebroventricular injection of $A\beta_{1\text{-}40}$ successfully induced learning and memory deficits in mice. Administration of s.c. 2 μg/kg and 10 μg/kg of NAP solution could decrease the escape latency of mice to a certain degree, which showed similar pattern to AD control group. NP/NAP could improve spatial memory in a dose-dependent manner. A dose of 2 μg/kg NP/NAP could slightly shorten the escape latency; and even at a high dose of 4 μg/kg, limited improvement was observed in spatial memory. Obvious improvement was observed in all three measurements of TGN-NP/NAP in a dose-dependent manner. The escape latency was apparently shortened on day 3, 4 and 5 with 1 μg/kg of TGN-NP/NAP. At a dose of 2 μg/kg, the escape latency was significantly decreased and close to that of Normal group, suggesting that the mice had learned the location of the platform completely. When the dose increased to 4 μg/kg, the escape latency was even slightly shorter than that of Normal group on day 5.

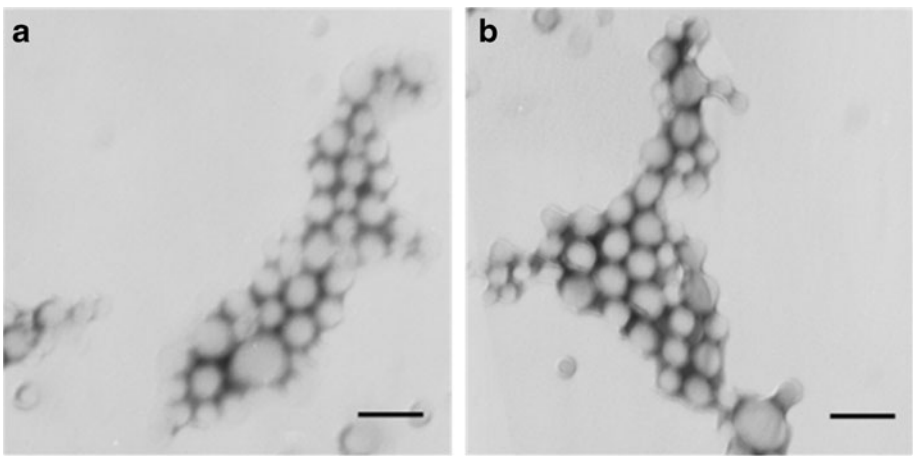

Fig. 1 Transmission electron micrograph of (**a**) NP/NAP and (**b**) TGN-NP/NAP, negatively stained with phosphotungstic acid solution. Bar=200 nm.

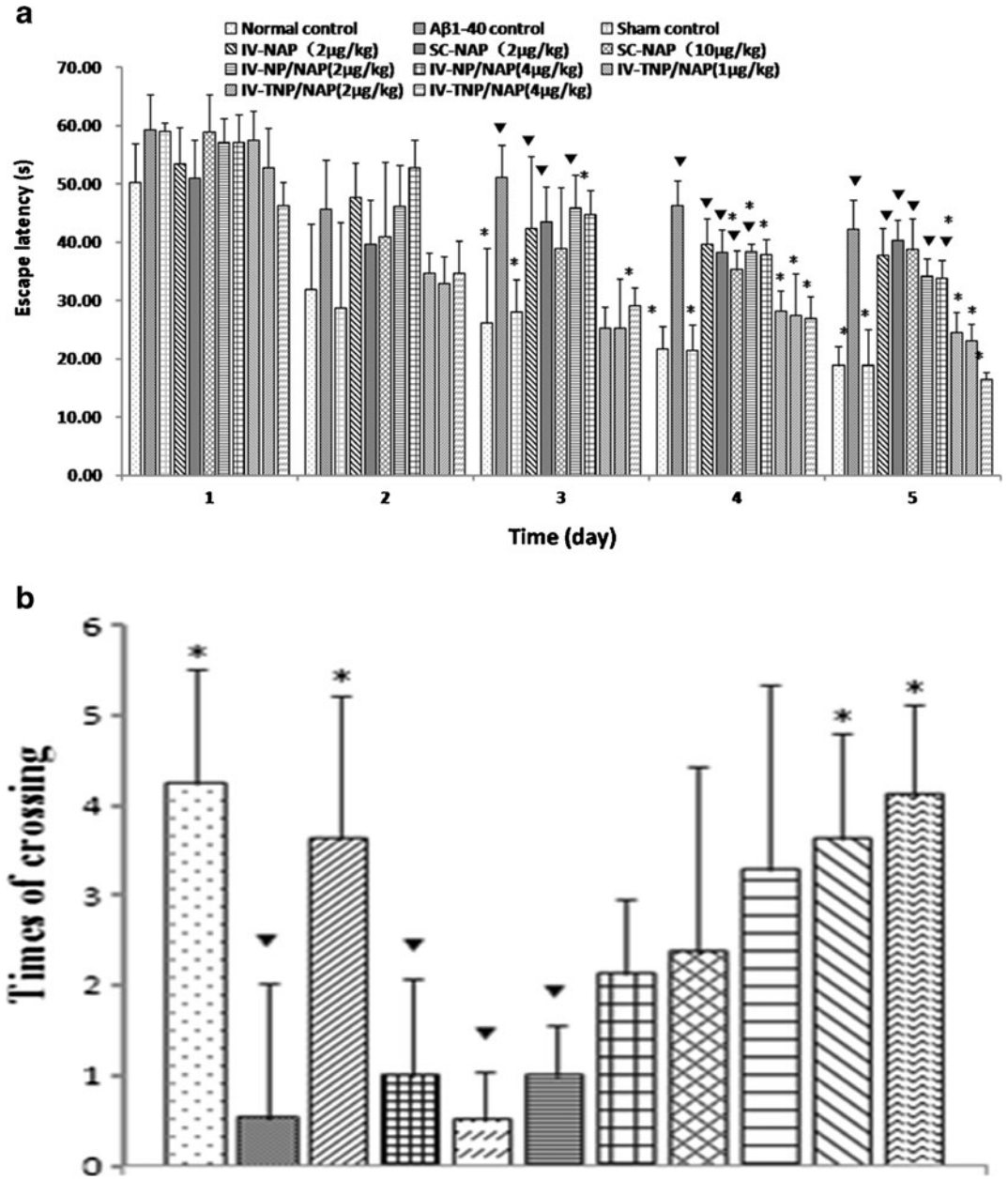

Fig. 2 Escape latency in hidden platform acquisition training (**a**) and the number of crossing of the removed-platform area in the probe test (**b**). Training began after 7 days of recovering and daily drug application. A spatial probe test performed with the platform removed at day 5. Data represented the mean±S.E.M. Normal control, $n=8$; AD control, $n=8$; Sham control, $n=8$; NAP solution i.v. (2 μg/kg), $n=7$; SC-NAP (2 μg/kg), $n=6$; SC-NAP (10 μg/kg) $n=7$; NP/NAP i.v. (2 μg/kg), $n=8$; NP/NAP i.v. (4 μg/kg), $n=8$; TGN-NP/NAP i.v. (1 μg/kg) $n=7$; TGN-NP/NAP i.v. (2 μg/kg) $n=8$; TGN-NP/NAP i.v. (4 μg/kg) $n=8$. *Asterisk* $p<0.001$, significantly different from AD control; *converted filled triangle* $p<0.001$, significantly different from normal control.

A probe test was performed 60 min after the last training trail, and the number of times crossing over the removed-platform area is displayed in Fig. 2b. The crossing number of the mice with memory deficits was recovered by treatment with TGN-NP/NAP in a dose response manner, with the highest platform crossing times observed at a dose of 4 μg/kg. By contrast, mice in Group D-I showed no significant differences with AD control group in the number of platform crossings. The similar results were observed in the paths of each group of mice in the probe test, shown in Fig. 3. Mice receiving TGN-NP/NAP (4 μg/kg) searched preferentially in the target quadrant, whereas mice in Group D-I had poorly focused search strategies.

AChE and ChAT Activity in Mouse Hippocampus and Cortex

Cholinergic system plays a crucial role in cognitive function. High levels of AChE in the brain are associated with

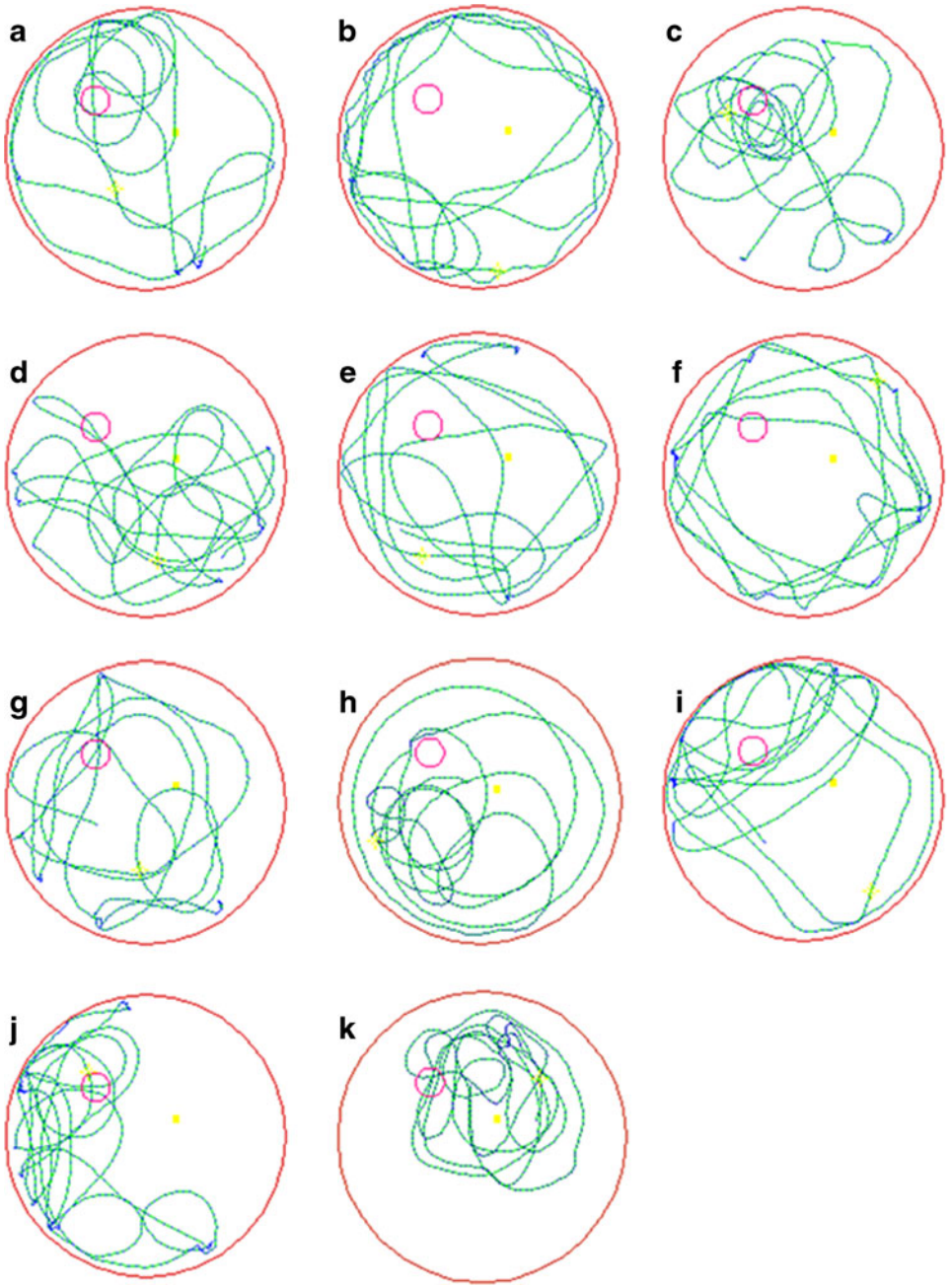

Fig. 3 The path of each group of mice in the probe test. A spatial probe test performed with the platform removed at day 5. The path of mice in the water maze during the 60 s was recorded. (**a**) Normal control; (**b**) AD control; (**c**) sham control; (**d**) NAP solution i.v. (2 $\mu g/kg$); (**e**) SC-NAP (2 $\mu g/kg$); (**f**) SC-NAP (10 $\mu g/kg$); (**g**) NP/NAP i.v. (2 $\mu g/kg$); (**h**) NP/NAP i.v. (4 $\mu g/kg$); (**i**) TGN-NP/NAP i.v. (1 $\mu g/kg$); (**j**) TGN-NP/NAP i.v. (2 $\mu g/kg$); (**k**) TGN-NP/NAP i.v. (4 $\mu g/kg$).

cognitive dysfunction (19). And decreased activity of ChAT, which is responsible for the synthesis of acetylcholine (Ach), is also observed in AD patients (20). In this study, we determined the AChE and ChAT activity in mouse hippocampus and cortex to help evaluate the effect of the formulations in the recognition memory improvement. The results of AChE activity (IU/g) in mouse hippocampus and cortex were shown in Fig. 4a and b. The activity of AChE of the mice in AD control group was significantly higher than that of Normal and Sham-operated groups in both hippocampus and cortex. The AChE activity decreased to the normal level after injection with TGN-NP/NAP formulation (Group I-K), which had significant differences with that of AD control group. The results revealed that TGN-NP/NAP had protective effect on the destroyed central cholinergic system. The activity of AChE in mice of Group D-H decreased to some extent, which still remained significantly higher than that of Normal and Sham-operated groups. The ChAT activity exhibited an opposing tendency (Fig. 4c and d), with the lowest value observed in AD control group. In comparison with other formulations (Group D-H), TGN-NP/NAP (Group I-K) could increase ChAT activity, and no

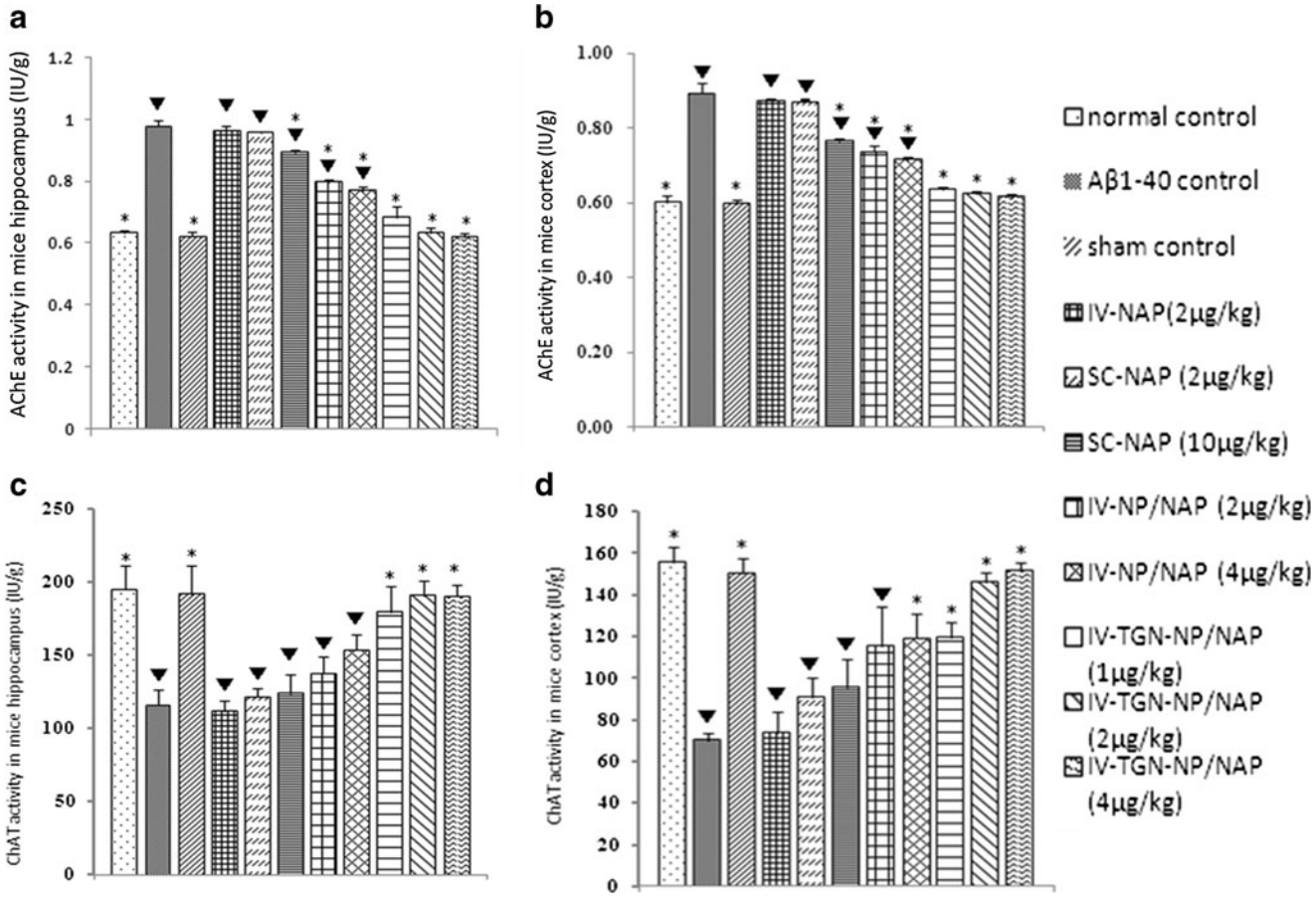

Fig. 4 AChE activity and ChAT activity in $A\beta_{1\text{-}40}$-treated mice hippocampus (**a**) and cortex (**b**). Data represented the mean±S.E.M. ($n=4$). *Asterisk* $p<0.001$, significantly different from AD control; $p<0.001$, significantly different from normal control.

significance was observed with that of Normal and Sham-operated groups, indicating that TGN-NP/NAP could reverse the reduced activity of ChAT induced by $A\beta_{1\text{-}40}$.

Histology

HE staining was conducted to evaluate the neuroprotective effect of the formulations. Compared with Normal and Sham-operated groups, mice in AD control group showed obvious damages in morphology and reduction in cells number of hippocampus (Fig. 5). The cell apoptosis of hippocampus in Group D-F was similar to that of AD control group, indicating that i.v. and s.c. of NAP solution had little neuroprotective effect. Compared with AD control group, pathological damages were slightly ameliorated in the mice receiving NP/NAP (Group G and H). No morphological damage was observed in the mice treated with TGN-NP/NAP, with high similarities to Normal and Sham-operated groups, indicating that encapsulation of NAP in TGN-NP could achieve a better protective effect on central nervous system.

The formation of Aβ plaques is a pathologic hallmark of AD (21). Congo red staining was used to assess Aβ plaque deposits in mouse hippocampus. No specific orange sediments could be seen in the slides of mice in both Normal and Sham-operated groups, while sediments were easily found in AD control group (Fig. 6). Mice in Group D-F displayed obvious plaques, which suggested that i.v. and s.c. of NAP solution had no improvement for Aβ plaques. NP/NAP (Group G and H) could ameliorate Aβ plaque deposits, but sediments still remained visible. Minimum detectable Aβ plaques could be observed at a dose of 1 μg/kg of TGN-NP/NAP, and there were no detectable Aβ plaques at the doses of 2 μg/kg and 4 μg/kg. These results demonstrated that higher doses of TGN-NP/NAP exhibited a better neuroprotective effect and had obvious suppression on the formation of Aβ plaque deposits in hippocampus.

DISCUSSION

A consensus sequence of TGNYKALHPHNG (denoted as Pep TGN) was obtained by four rounds of *in vivo* phage display screening in previous study. Phage clones displaying

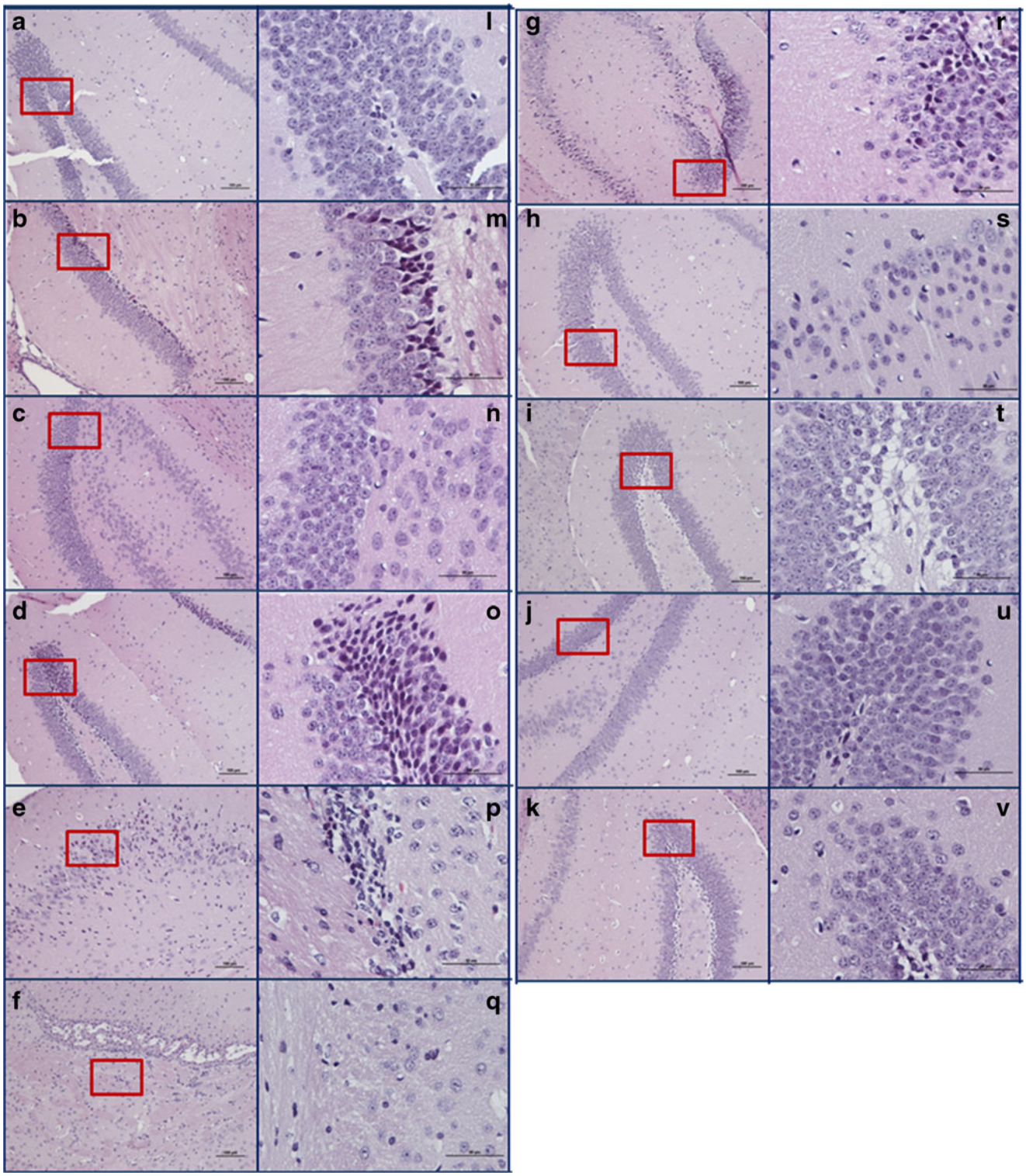

Fig. 5 Representative images of HE staining. Numerous neuronal cells in the $A\beta_{1\text{-}40}$ control group were damaged by toxicity induced by the $A\beta_{1\text{-}40}$ aggregates. TGN-NP/NAP treatment significantly reduced the number of damaged neuronal cells. (**a**, **l**) Normal control group; (**b**, **m**) AD control group; (**c**, **n**) Sham control group; (**d**, **o**) NAP solution i.v. (2 μg/kg); (**e**, **p**) SC-NAP (2 μg/kg); (**f**, **q**) SC-NAP (10 μg/kg); (**g**, **r**) NP/NAP i.v. (2 μg/kg); (**h**, **s**) NP/NAP i.v. (4 μg/kg); (**i**, **t**) TGN-NP/NAP i.v. (1 μg/kg); (**j**, **u**) TGN-NP/NAP i.v. (2 μg/kg); (**k**, **v**) TGN-NP/NAP i.v. (4 μg/kg). (**l**–**v**) (Bar=50 μm) are higher magnification images of the *boxed areas* in (**a**–**k**) (Bar=100 μm).

Pep TGN revealed a significant superiority on brain transport efficiency. When conjugated to the surface of PLGA nanoparticles, Pep TGN facilitated the delivery of nanoparticles across the BBB. Therefore, we employed TGN

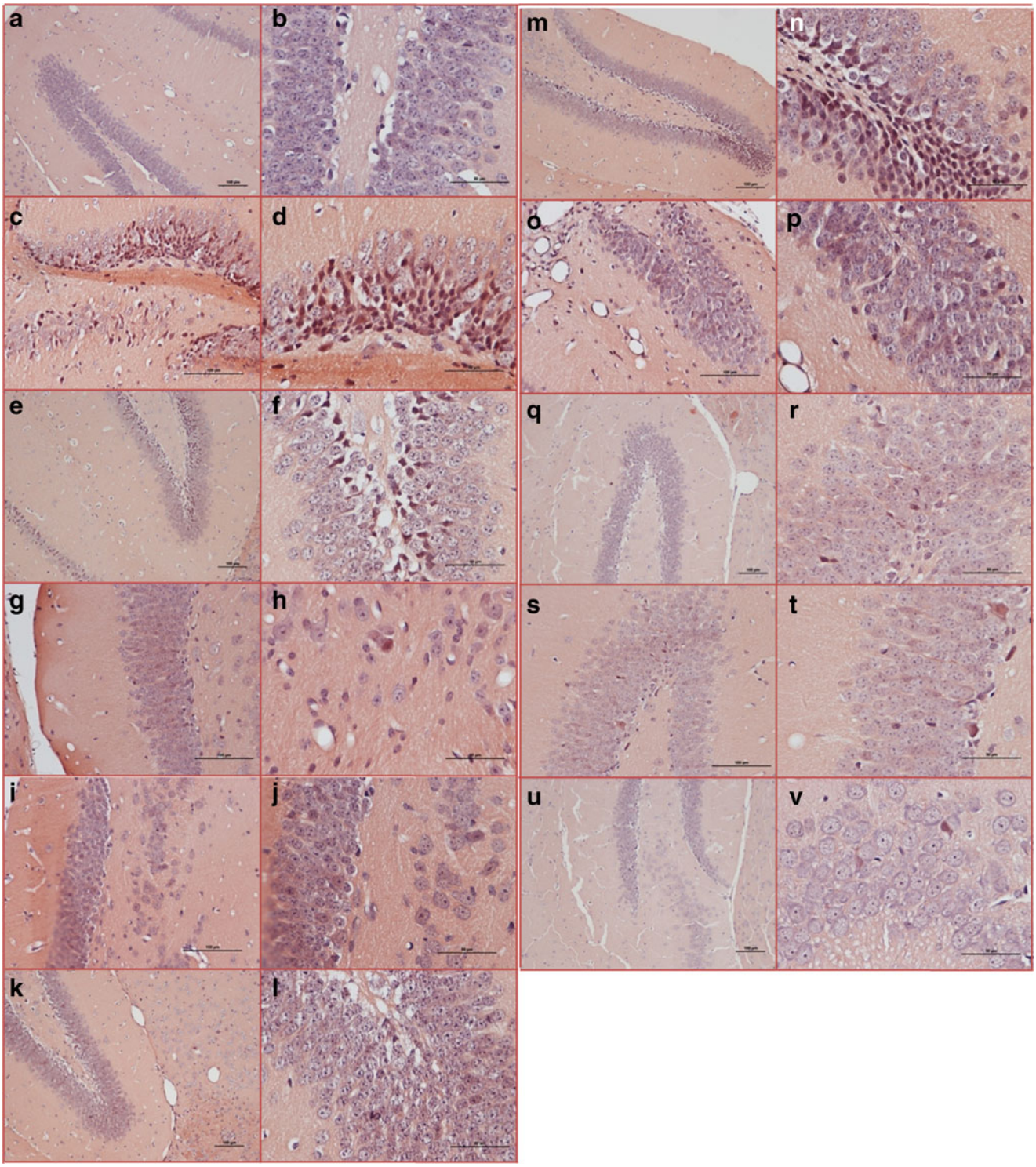

Fig. 6 Representative images of Aβ staining. Numerous neuronal cells in the $A\beta_{1\text{-}40}$ control group were damaged by toxicity induced by the Aβ1-40 aggregates. TGN-NP/NAP treatment significantly reduced the number of Aβ-positive staining cells. (**a**, **b**) Normal control group; (**c**, **d**) AD control group; (**e**, **f**) sham control group; (**g**, **h**) NAP solution i.v. (2 μg/kg); (**i**, **j**) SC-NAP (2 μg/kg); (**k**, **l**) SC-NAP (10 μg/kg); (**m**, **n**) NP/NAP i.v. (2 μg/kg); (**o**, **p**) NP/NAP i.v. (4 μg/kg); (**q**, **r**) TGN-NP/NAP i.v. (1 μg/kg); (**s**, **t**) TGN-NP/NAP i.v. (2 μg/kg); (**u**, **v**) TGN-NP/NAP i.v. (4 μg/kg) (Bar=100 μm).

as a targeting motif in this study to deliver neuroprotective peptides into brain.

NAP, an eight amino peptide, is able to inhibit $A\beta_{1\text{-}40}$ fibril formation at a wide concentration range (10^{-17} to 10^{-10}) and

has protection against toxicity associated with the β-amyloid peptide in cell culture. This is the first work on neuroprotective bioactivity of NAP entrapped in brain-targeting nanoparticles modified with phage-displayed peptide. $A\beta_{1\text{-}40}$ aggregate-injured mice were chosen as animal model for the evaluation of therapeutic efficacy of NAP -loaded TGN-NP. It has been reported $A\beta_{1\text{-}40}$ can form amyloid-like fibrils *in vitro*, which plays an important role in the pathogenesis of Alzheimer's disease. An acute infusion of $A\beta_{1\text{-}40}$ aggregates into the brain could cause brain dysfunction, evidenced by neurodegeneration and an impairment of learning and memory (22). In this study, microinjection of aggregated $A\beta_{1\text{-}40}$ also simulated AD behaviors and pathological features in AD model group compared with normal control group and sham-operated group. Thus AD model was successfully established.

According to the behavioral research and biochemical indicators results, direct administration of NAP solution (2 μg/kg) intravenously or subcutaneously had no improvement on $A\beta_{1\text{-}40}$ induced AD model mice. Even when the dose was five times higher (10 μg/kg) via subcutaneous administration, the improvement of memory and biochemical indicators was still limited. Poor amelioration in the mice memory deficits was observed in NP/NAP group at the dose of 4 μg/kg of NAP, suggesting that entrapment of NAP in PEG-PLGA nanoparticles only contributed to the stability and the release property of NAP *in vivo*. Administration of NAP-loaded TGN-NP at the dose of 1 μg/kg of NAP showed better neuroprotective effect than intravenous or subcutaneous administration of NAP solution. When the dose of TGN-NP was increased to 2 μg/kg or 4 μg/kg, the latency was shortened significantly and the AChE and ChAT activity recovered to the normal level. The deposition of $A\beta_{1\text{-}40}$ was significantly reduced, and the loss of neurons in hippocampus also obviously decreased in the NAP loaded TGN-NP, suggesting that TGN-NP had an apparent neuroprotective effect in the mice model.

Directly administration of NAP solution could not result in any amelioration either in behavior study or AChE and ChAT activity, which was probably caused by easy degeneration of NAP by enzymes *in vivo*. The protein drugs can be protected from enzymatic degradation when loaded in the PEG-PLGA nanoparticles, while the phage-displayed peptide can mediate the entrance of drug-loading nanoparticles into the brain, thus improving the treatment of brain diseases. The protection in NAP delivery to the brain achieved by TGN-NP was consistent with our previous results relating to enhancement in brain drug delivery of TGN modified nanoparticles.

CONCLUSION

In conclusion, TGN modified PEG-PLGA nanoparticles could protect peptide drugs like NAP from enzymes *in vivo*, and effectively mediate NAP transport into the brain following intravenous administration in mice. These results demonstrated that TGN-NP is a promising drug delivery system for protein drugs to cross BBB and play their therapeutic role in the central nervous system.

ACKNOWLEDGMENTS AND DISCLOSURES

Jingwei Li and Chi Zhang contributed equally to this work. This work was supported in part by grants from the National Basic Research Program of China (973 Program) (2007CB935800), National Science and Technology Major Project 2009ZX09310-006, National Natural Science Foundation of China NO.81072592 and Doctorial Innovation Fund of Fudan University.

REFERENCES

1. 2011 Alzheimer's disease facts and figures. Alzheimer's and Dementia: Alzheimer's Association; 2011;7(2):208–24.
2. De Rosa R, Garcia AA, Braschi C, Capsoni S, Maffei L, Berardi N, *et al.* Intranasal administration of nerve growth factor (NGF) rescues recognition memory deficits in AD11 anti-NGF transgenic mice. Proc Natl Acad Sci U S A. 2005;102(10):3811–6. 2005-03-08.
3. Nagahara AH, Bernot T, Moseanko R, Brignolo L, Blesch A, Conner JM, *et al.* Long-term reversal of cholinergic neuronal decline in aged non-human primates by lentiviral NGF gene delivery. Exp Neurol. 2009;215(1):153–9. 2009-01-01.
4. Wang ZL, Cheng SM, Ma MM, Ma YP, Yang JP, Xu GL, *et al.* Intranasally delivered bFGF enhances neurogenesis in adult rats following cerebral ischemia. Neurosci Lett. 2008;446(1):30–5. 2008-11-28.
5. Lobner D, Ali C. Mechanisms of bFGF and NT-4 potentiation of necrotic neuronal death. Brain Res. 2002;954(1):42–50. 2002-11-01.
6. Gozes I. Activity-dependent neuroprotective protein: from gene to drug candidate. Pharmacol Ther. 2007;114(2):146–54. 2007-05-01.
7. Pinhasov A, Mandel S, Torchinsky A, Giladi E, Pittel Z, Goldsweig AM, *et al.* Activity-dependent neuroprotective protein: a novel gene essential for brain formation. Brain Res Dev Brain Res. 2003;144(1):83–90. 2003-08-12.
8. Poggi SH, Goodwin K, Hill JM, Brenneman DE, Tendi E, Schinelli S, *et al.* The role of activity-dependent neuroprotective protein in a mouse model of fetal alcohol syndrome. Am J Obstet Gynecol. 2003;189(3):790–3. 2003-09-01.
9. Bassan M, Zamostiano R, Davidson A, Pinhasov A, Giladi E, Perl O, *et al.* Complete sequence of a novel protein containing a femtomolar-activity-dependent neuroprotective peptide. J Neurochem. 1999;72(3):1283–93. 1999-03-01.
10. Beni-Adani L, Gozes I, Cohen Y, Assaf Y, Steingart RA, Brenneman DE, *et al.* A peptide derived from activity-dependent neuroprotective protein (ADNP) ameliorates injury response in closed head injury in mice. J Pharmacol Exp Ther. 2001;296(1):57–63. 2001-01-01.
11. Zemlyak I, Manley N, Sapolsky R, Gozes I. NAP protects hippocampal neurons against multiple toxins. Peptides. 2007;28(10):2004–8. 2007-10-01.

12. Alcalay RN, Giladi E, Pick CG, Gozes I. Intranasal administration of NAP, a neuroprotective peptide, decreases anxiety-like behavior in aging mice in the elevated plus maze. Neurosci Lett. 2004;361(1–3):128–31. 2004-05-06.
13. Divinski I, Holtser-Cochav M, Vulih-Schultzman I, Steingart RA, Gozes I. Peptide neuroprotection through specific interaction with brain tubulin. J Neurochem. 2006;98(3):973–84. 2006-08-01.
14. Gozes I, Alcalay R, Giladi E, Pinhasov A, Furman S, Brenneman DE. NAP accelerates the performance of normal rats in the water maze. J Mol Neurosci. 2002;19(1–2):167–70. 2002-08-01.
15. Gozes I, Morimoto BH, Tiong J, Fox A, Sutherland K, Dangoor D, *et al.* NAP: research and development of a peptide derived from activity-dependent neuroprotective protein (ADNP). Cns Drug Rev. 2005;11(4):353–68. 2005-06-01.
16. Matsuoka Y, Gray AJ, Hirata-Fukae C, Minami SS, Waterhouse EG, Mattson MP, *et al.* Intranasal NAP administration reduces accumulation of amyloid peptide and tau hyperphosphorylation in a transgenic mouse model of Alzheimer's disease at early pathological stage. J Mol Neurosci. 2007;31(2):165–70. 2007-01-20.
17. Li J, Feng L, Fan L, Zha Y, Guo L, Zhang Q, *et al.* Targeting the brain with PEG-PLGA nanoparticles modified with phage-displayed peptides. Biomaterials. 2011;32(21):4943–50. 2011-07-01.
18. Sureda FX, Gutierrez-Cuesta J, Romeu M, Mulero M, Canudas AM, Camins A, *et al.* Changes in oxidative stress parameters and neurodegeneration markers in the brain of the senescence-accelerated mice SAMP-8. Exp Gerontol. 2006;41(4):360–7. 2006-04-01.
19. de Freitas RM. Lipoic Acid increases hippocampal choline acetyltransferase and acetylcholinesterase activities and improvement memory in epileptic rats. Neurochem Res. 2010;35(1):162–70. 2010-01-01.
20. Park D, Lee HJ, Joo SS, Bae DK, Yang G, Yang YH, *et al.* Human neural stem cells over-expressing choline acetyltransferase restore cognition in rat model of cognitive dysfunction. Exp Neurol. 2012;234(2):521–6. 2012-04-01.
21. Wang H, He J, Zhang R, Zhu S, Wang J, Kong L, *et al.* Sensorimotor gating and memory deficits in an APP/PS1 double transgenic mouse model of Alzheimer's disease. Behav Brain Res. 2012;233(1):237–43. 2012-07-15.
22. Lauren J, Gimbel DA, Nygaard HB, Gilbert JW, Strittmatter SM. Cellular prion protein mediates impairment of synaptic plasticity by amyloid-beta oligomers. Nature. 2009;457(7233):1128–32. 2009-02-26.